Supporting information for

Understanding the Performance of a Bisphosphonate Ru Water Oxidation Catalyst

Jesús A. Luque-Urrutia,[‡] Jayneil M. Kamdar,[§] Douglas B. Grotjahn,[§,*] Miquel Solà,[‡,*] and Albert Poater[‡,*]

[‡]Institut de Química Computacional i Catàlisi and Departament de Química, Universitat de Girona, C/ Maria Aurèlia Capmany 69, 17003 Girona, Catalonia, Spain.

[§]Department of Chemistry and Biochemistry, San Diego State University, 5500 Campanile Drive, San Diego, CA, US 92182-1030.

Table of Contents

pK_a calculation. Equations and explanation.

We begin with a general reaction:

$$AOH \rightarrow AO^- + H^+$$

Which will give us a ΔG. This can be used in the pKa calculation as follows:

$$\Delta G = -R \cdot T \cdot ln(K_a)$$

$$pK_a = log(e^{\frac{\Delta G}{RT}})$$

This is how we obtain our calculated pK_a. In order to have a better approximation, we follow the same procedure as Concepcion et al. have presented in their SI by calculating different pKa and comparing them with known experimental values in order to adjust our results:

Table *S1*. Experimental, DFT and corrected pKa values for different acids.

Acid	pK_a		
	Experimental	Calculated	Corrected
CF_3-COOH	0.23	3.1	0.17
CHF_2-COOH	1.34	5.3	1.08
CH_2F-COOH	2.60	9.1	2.56
CH_3-COOH	4.76	14.2	4.61
H-PO(OH)$_2$	1.30	6.4	1.52
H_3C-PO(OH)$_2$	2.38	9.3	2.66

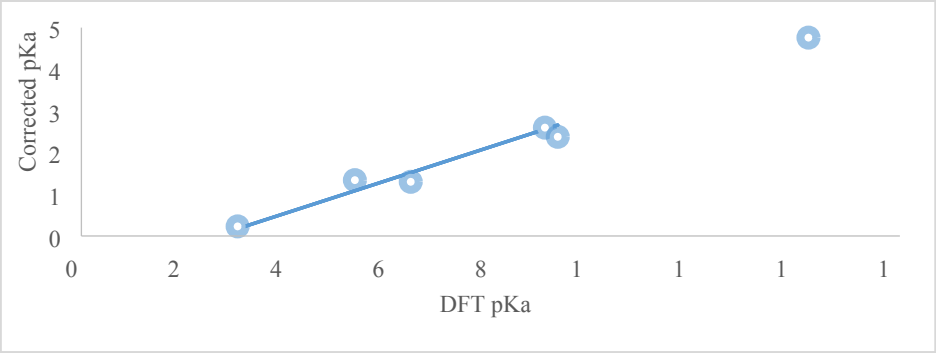

Figure S1. Plot of the DFT (x-axys) and experimental (y-axys) pKa of the different

By using the formula obtained in the linear regression, we can adjust our DFT pKa to be closer to the experimental ones.

Reduction potentials. Equations and explanation

Starting from the reduction potential formula explained in the article:

$$\varepsilon^{o}_{red} = -\frac{\Delta G_{reaction}}{-nF} - SHE$$

We can specify our ΔG according to a PCET reaction:

$$M^{III}OH + H^+ + e^- \rightarrow M^{II}OH_2$$

Therefore, we obtain the following ΔG:

$$\Delta G_{reaction} = \Delta G_{M^{II}OH_2} - \Delta G_{M^{III}OH} - \Delta G_{H^+}$$

To address the new proton term, respect to a redox reaction which does not appear, we can observe the Standard Hydrogen Electrode reaction:

$$H^+_{solv} + e^- \rightarrow \frac{1}{2} \cdot H_{2gas}$$

Which we can obtain the ΔG_{SHE}:

$$\Delta G_{SHE} = \frac{1}{2}\Delta G_{H_2} - \Delta G_{H^+}$$

Where we can obtain the ΔG_{H^+} which we can translate into our $\Delta G_{reaction}$:

$$\varepsilon^{o}_{red} = -\frac{\Delta G_{M^{II}OH_2} - \Delta G_{M^{III}OH} - \frac{1}{2}\Delta G_{H_2} + \Delta G_{SHE}}{-nF} - SHE$$

$$\varepsilon^{o}_{red} = -\frac{\Delta G_{M^{II}OH_2} - \Delta G_{M^{III}OH} - \frac{1}{2}\Delta G_{H_2}}{-nF} + SHE - SHE$$

And thus, we obtain the proposed reaction for the reduction potential for PCETs reactions.

$$\varepsilon^{o}_{red} = -\frac{\Delta G_{M^{II}OH_2} - \Delta G_{M^{III}OH} - \frac{1}{2}\Delta G_{H_2}}{-nF}$$

In order to compare it with the more used methodology of using the $\Delta G_{reaction}$ with an experimental $\Delta G_{H^+} = 270.3\ kcal/mol$; we performed both and obtained the same potentials in both cases, being able to use any of them. However, due to not requiring experimental values and because we are trying to address the potentials from a computational point of view, we used the methodology explained above.

Finally, in order to predict the involvement of protons in the redox potentials we use the Nernst equation correction:

$$\varepsilon_{red} = \varepsilon^{o}_{red} + 0.059 \cdot (pH - pKa)$$

Given the following pKa:

$$MOH_2^{3+}: pKa^I \quad \& \quad MOH_2^{2+}: pKa^{II}$$

If $pH < pKa^I$ we consider a $0H^+/1e^-$ pH independent reaction:

$$M^{III}OH_2^{3+} + e^- \rightarrow M^{II}OH_2^{2+}$$

Thus no correction is applied.

If $pKa^I < pH < pKa^{II}$ we consider a $1H^+/1e^-$ pH dependent reaction:

$$M^{III}OH^{2+} + e^- + H^+ \rightarrow M^{II}OH_2^{2+}$$

Thus the Nernst equation is used.

If $pKa^{II} < pH$ then we consider a $0H^+/1e^-$ pH independent reaction:

$M^{III}OH^{2+} + e^- \rightarrow M^{II}OH^+$

Thus no correction is applied.

Full figures at pH=8 and pH=1.

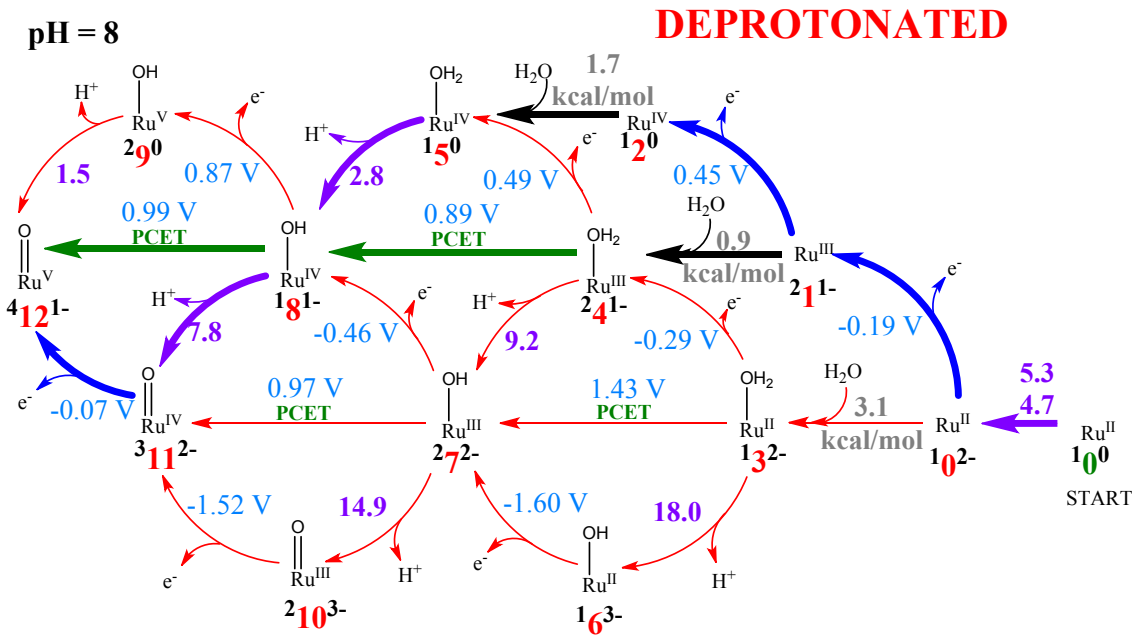

Figure S2. Mechanism for the bisphosphonate Ru catalyst **B** according to the protonation of the two phosphonate ligands at pH = 8. Species $^{1}\mathbf{0}^{2-}$ is **B** deprotonated twice at pH 8; the superscripts left and right signify spin multiplicity (here, singlet) and overall charge, respectively. For reaction arrows, red = less favorable, blue = oxidation, green = PCET, and purple = deprotonation. For numbered species, green indicates deprotonated diphosphonate ligand, whereas red indicates doubly deprotonated ligand. Numbers near arrows in blue indicate the reduction potential in V, purple numbers indicate pK_a and grey numbers (minima) indicate Gibbs free energy in kcal/mol.

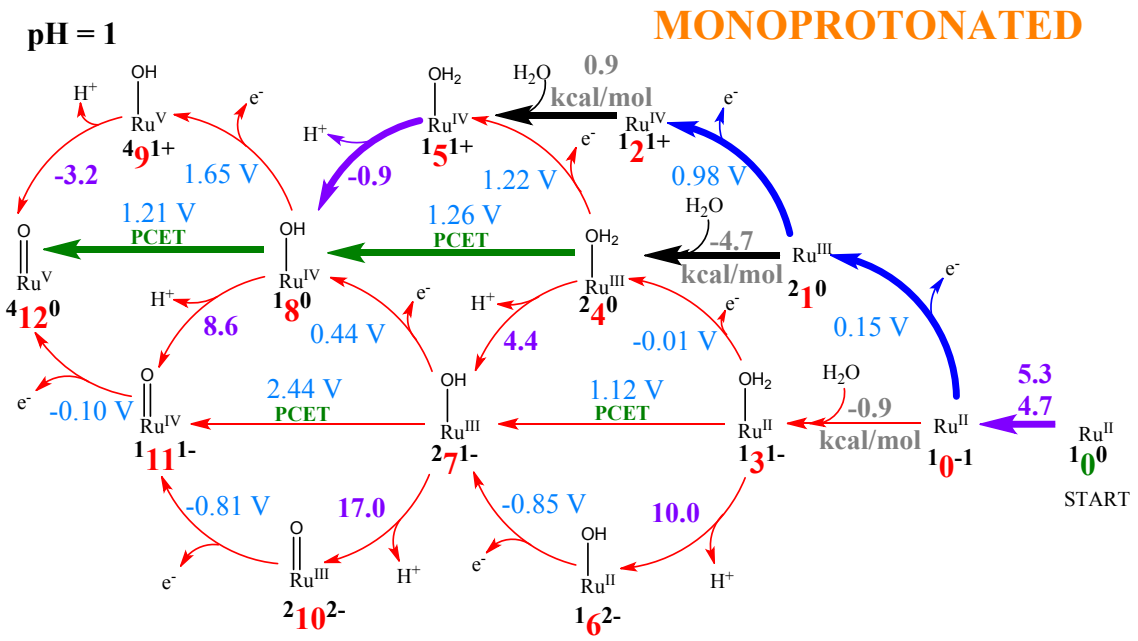

Figure S3. Mechanism for the bisphosphonate Ru catalyst **B** with retention of ligand protons at pH 1. For reaction arrows, red = less favorable, blue = oxidation, green = PCET, and purple = deprotonation. For numbered species, green indicates deprotonated diphosphonate ligand, whereas red indicates doubly deprotonated ligand. Numbers near arrows indicate the reduction potential in V, purple numbers indicate pKa and grey numbers (minima) indicate Gibbs free energy in kcal/mol.

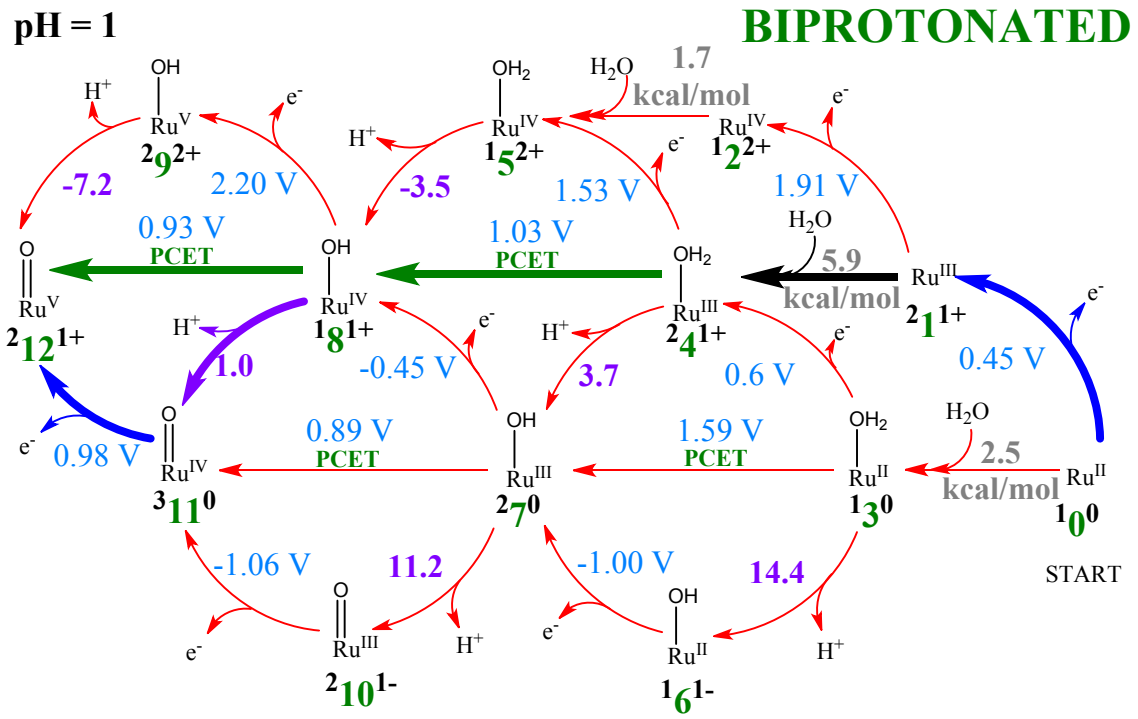

Figure S4. Mechanism for the bisphosphonate Ru catalyst **B** with retention of ligand protons at pH 1. For reaction arrows, red = less favorable, blue = oxidation, green = PCET, and purple = deprotonation. For numbered species, green indicates deprotonated diphosphonate ligand, whereas red indicates doubly deprotonated ligand. Numbers near arrows indicate the reduction potential in V, purple numbers indicate pKa and grey numbers (minima) indicate Gibbs free energy in kcal/mol.

Table S2. pK_a for the conversion of the two phosphonates in the catalyst: biprotonated, monoprotonated and deprotonated.

Biprotonated to Monoprotonated	pKa	Monoprotonated to Deprotonated	pKa
Bi-0 to Mono-0	5.3	Mono-0 to Dep-0	4.7
Bi-1 to Mono-1	3.3	Mono-1 to Dep-1	2.3
Bi-2 to Mono-2	-2.9	Mono-2 to Dep-2	-1.2
Bi-3 to Mono-3	4.3	Mono-3 to Dep-3	5.8
Bi-4 to Mono-4	0.2	Mono-4 to Dep-4	4.0
Bi-5 to Mono-5	-1.8	Mono-5 to Dep-5	-1.0
Bi-6 to Mono-6	-0.1	Mono-6 to Dep-6	13.9
Bi-7 to Mono-7	0.9	Mono-7 to Dep-7	8.8
Bi-8 to Mono-8	0.8	Mono-8 to Dep-8	2.8
Bi-9 to Mono-9	-2.9	Mono-9 to Dep-9	-2.5
Bi-10 to Mono-10	6.7	Mono-10 to Dep-10	6.7
Bi-11 to Mono-11	8.3	Mono-11 to Dep-11	2.0
Bi-12 to Mono-12	1.1	Mono-12 to Dep-12	2.2

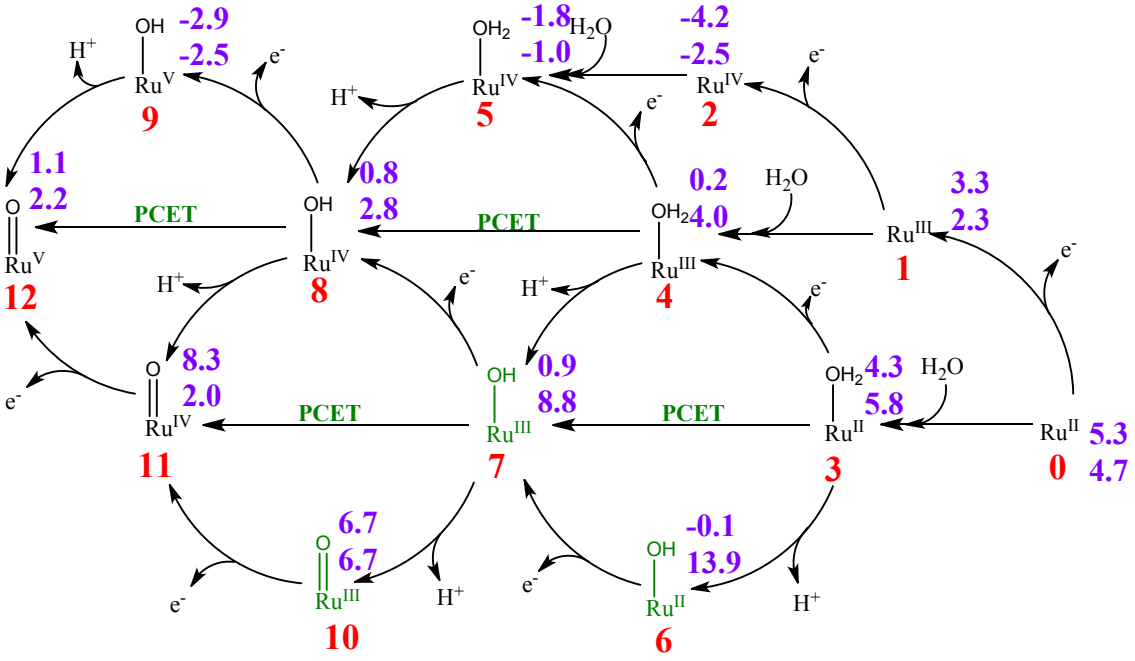

Figure S5. pK_a for each molecule going from Biprotonated to Monoprotonated and Deprotonated phosphonates.

Table S3. Multiplicity for all the relevant structures.

	0		1		2		3		4		5		6		7	
	M	S^2	M	S^2	M	S^2	M	S^2	M	S^2	M	S^2	M	S^2	M	S^2
Bip.	R.S	0	D	0.76	R.S	0	R.S	0	D	0.76	R.S	0	R.S	0	D	0.76
Monop.	R.S	0	D	0.76	R.S	0	R.S	0	D	0.76	R.S	0	R.S	0	D	0.76
Dep.	R.S	0	D	0.76	R.S	0	R.S	0	D	0.76	R.S	0	R.S	0	D	0.76
	8		9		10		11		12		Adduct		TS I2M		TS WNA	
	M	S^2	M	S^2	M	S^2	M	S^2	M	S^2	M	S^2	M	S^2	M	S^2
Bip.	R.S	0	D	0.76	D	0.76	T	2	D	0.76	U.S	1.04	R.S	0	D	0.76
Monop.	R.S	0	Q	3.77	D	0.76	R.S	0	Q	3.76	-	-	-	-	-	-
Dep.	R.S	0	D	0.76	D	0.76	T	2	Q	3.76	U.S	1.02	R.S	0	D	0.76

Experimental voltammetries

The following are taken from Grotjahn et. al. *ChemCatChem* **2016**, *8*, 3045-3049 :

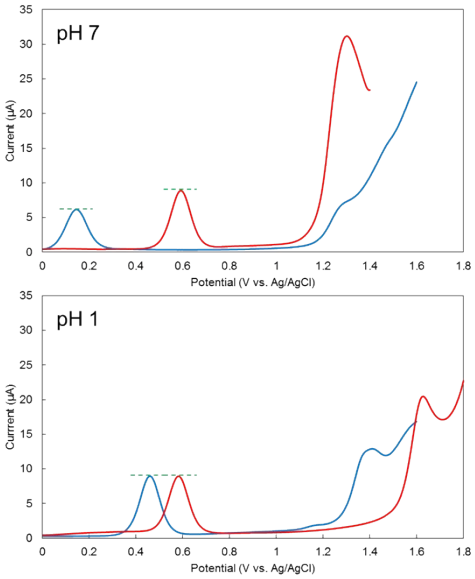

Figure S6: Differential pulse voltammetry comparing **2** (blue) and **3** (red). {Note: **2** is the bpa catalyst subject of our computational studies} Top: pH 7 (0.1 M potassium phosphate buffer). Bottom: pH 1 (0.1 M CF3SO3H). Dashed lines highlight relative peak heights. Catalyst concentration: 0.5 mM.

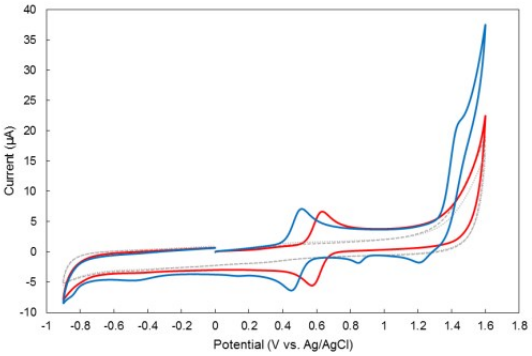

Figure S7. Cyclic voltammetry of Ru(bpa) at pH=1 (Blue)

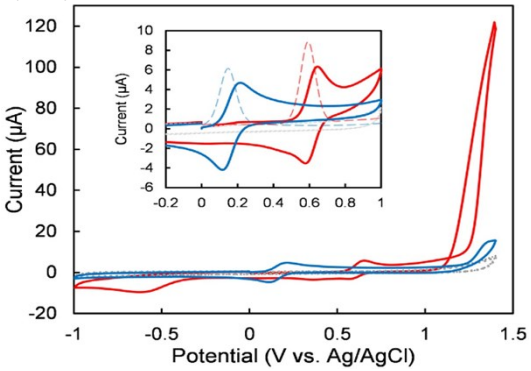

Figure S8. Cyclic voltammetry of Ru(bpa) at pH=7 (Blue)

And the following is taken from Xie et al. *Angew. Chem. Int. Ed.* **2016**, *55*, 8067:

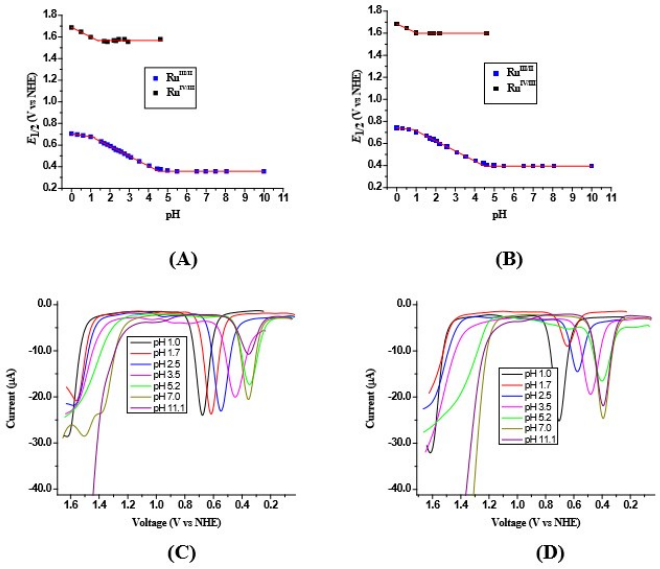

Figure S9: Pourbaix diagrams and square wave voltammograms for $[Ru^{II}(bpaH_2)(pic)_2]$ **(A,C)**; $[Ru^{II}(bpaH_2)(isq)_2]$ **(B,D)**.

CERIUM AMMONIUM NITRATE STUDY

Currently, there is no known structure for Cerium Ammonium Nitrate in aqueous solution. We did try to develop a robust guess of CAN by trying to emulate a redox reaction of 1.6~1.7V in order to evaluate possible dimerizations between the Ru catalyst and the Ce in CAN, as there are other articles like Costas and Lloret-Fillol[1] that propose such a coordination. Nevertheless, after several trials and exchanges between other researchers in the field, we concluded that we do not hold a solid ground in our CAN structure hypothesis to use it for the mechanism. Rather than proposing a theoretical mechanism with Ru-Ce that might or might not be correct, we decided not to include it into the report. Here we show a sample of the tests done for CAN, and they will be included in the SI as well. Calculations for CAN have been performed with 6-31++G** to include diffuse functions, and NO_3^- leaves through the following formula:

$$\left(Ce(NO_3)_6\right)^{-2} + 3{\cdot}H_2O \rightarrow Ce(NO_3)_5^{-} + \left(NO_3{\cdot}3H_2O\right)^{-}$$

[1] Design of Iron Coordination Complexes as Highly Active Homogenous Water Oxidation Catalysts by Deuteration of Oxidation-Sensitive Sites *J. Am. Chem. Soc.* **2019**, *141*, 1, 323-333

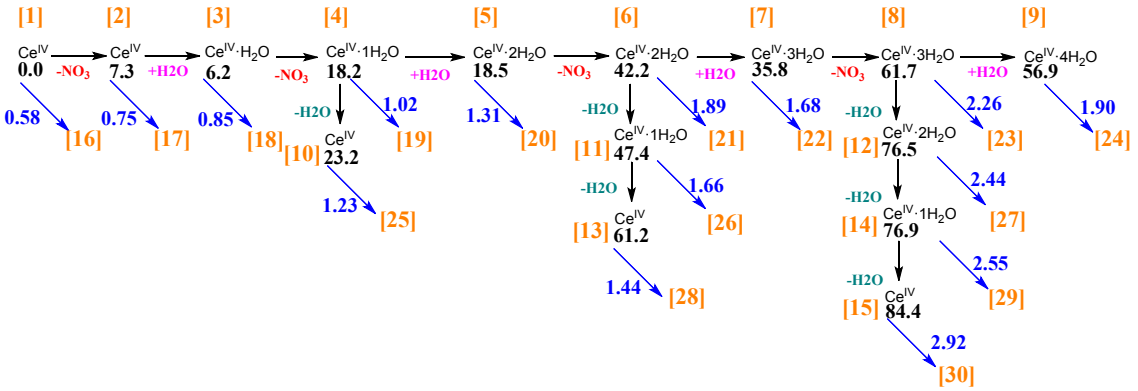

Figure S10. Cerium Ammonium Nitrate electropotential study (in blue there are the reduction potentials; in black the Gibbs free energies).